JOURNAL OF CATALYSIS 4, 685–690 (1965)

Multilayer Nitrogen Adsorption in Porous Structures

JOHN B. BUTT

From the Department of Engineering and Applied Science
Yale University, New Haven, Connecticut

Received February 24, 1965; revised April 29, 1965

The results of volume–area distribution calculations are sensitive functions of the correlation of adsorbed multilayer thickness employed in the computation. Disagreement between correlations proposed appears due primarily to the fact that the effects of pore structure on the adsorption are not included.

The present work presents a correlation of multilayer nitrogen adsorption in porous structures which is based on reported isotherms for a wide range of pore systems. The consistency of surface area results obtained from computations employing the correlation is demonstrated.

Introduction

A number of methods have been devised for determination of volume–area distributions within porous structures from nitrogen adsorption–desorption isotherms under specified conditions (*1*, *2*, *3*, *4*). Although the basic theory involved in each is essentially the same, application of various methods to the same isotherm data often results in differing shapes of distribution curves and different cumulative surface area values. These discrepancies are almost entirely due to the different correlations for the thickness of the adsorbed layer of nitrogen which are employed in the several methods (*5*).

The multilayer thickness correlation is involved directly in the distribution calculation through its appearance as a correction to the Kelvin radius. For conditions and properties pertaining to nitrogen adsorption at the normal boiling point, capillary radius is given by

$$R_c = R_k + t = -(4.05/\log_{10} X) + t \quad (1)$$

Discrepancies in the multilayer thickness correlation appear directly in this relationship. The numerous assumptions involved in application of the Kelvin relationship to pore sizes of the order of molecular dimensions require arguments concerning the nature of distribution relationships in this region to be qualitative. Due to the cumulative nature of the computations required by most methods, however, the errors are cumulative and distributions in the small micropore region will reflect discrepancies arising at much larger pore sizes, with resultant large effects on properties estimated from the distribution. The present work is directed toward relating the effect of porous structure on the multilayer adsorption of nitrogen.

Notation

a	Constant of Eq. (2)
a'	Constant of Eq. (5)
N	Number of adsorbed monolayers
n	Constant of Eq. (2)
R_c	Capillary radius effective (Å)
R_k	Kelvin radius (Å)
$\bar{r}$	Average radius $= 2V_g/S_{BET}$
S_{ads}	Surface area computed from adsorption branch of isotherm (m^2/gm)
S_{BET}	Surface area computed from BET equation (m^2/g)
S_{des}	Surface area computed from desorption branch of isotherm (m^2/g)
t	Thickness of adsorbed multilayer (Å)
V_g	Volume adsorbed at unity relative pressure (cc/g)
X	Relative pressure
X_m	Relative pressure at monolayer coverage

Physical Adsorption of Nitrogen

Of particular interest to this work are the correlations of nitrogen adsorption reported by Shull (*6*), Pierce (*7*), Cranston and Inkley (*8*), Mingle and Smith (*9*), Lippens, Linsen, and deBoer (*10*), and Halsey (*11*). The first three of these correlations are based on nitrogen adsorption data on nonporous solids; data based on observations with porous materials are given by Mingle and Smith, and Lippens *et al.* It is reasonable to expect that porous structure can significantly affect the apparent relationship between multilayer thickness and relative pressure; evidence of this is provided by the disagreement among the various relationships which have been proposed.

Mingle and Smith have suggested that a Halsey-type expression

$$N = a[\ln (1/X)]^{-1/n} \qquad (2)$$

might be applied successfully to correlation of observed adsorption data for porous solids if the constants a and n could be related to properties characteristic of the structure. This equation has been employed for distribution computations in the form (*3*)

$$N = \left[\frac{5}{\ln (1/X)}\right]^{1/3} \qquad (3)$$

The values of N predicted by Eq. (3), however, are considerably larger (> 15%) than those given by other correlations except for $X > 0.8$; it has been concluded that while the form of the Halsey relationship may be suitable, the constants employed in Eq. (3) are not adequate for representation of nitrogen adsorption on porous materials (*5*). On the other hand, it has also been shown that the correlation developed by Mingle and Smith on the basis of Eq. (2) fails badly for at least one type of porous structure. The reasons for this are attributed to difficulties in developing the correlation (only a few isotherm determinations with little independent information concerning the nature of the porous structure of the solids studied) rather than to the approach, but the result is that the utility of Eq. (2) in analysis of multilayer nitrogen adsorption according to their suggestions has not been established quantitatively.

The recent data reported by deBoer and co-workers (*10, 12–14*), experimental adsorption–desorption isotherms together with considerable independent information concerning the nature of the porous structures involved, provide a sound basis for a more quantitative study of pore structure effects on adsorption.

Effects of Pore Structure

The constant, a, of Eq. (2) may be evaluated in part from the fact that the relationship should correctly express monolayer coverage. For a value of $N = 1$

$$a = [\ln (1/X)_m]^{1/n} \qquad (4)$$

This expression pertains to ideal monolayer coverage on a flat surface. For a nonideal case

$$a = a'[\ln (1/X)_m]^{1/n} \qquad (5)$$

in which a' may vary from unity due to surface curvature and other effects. Combining Eqs. (2) and (5)

$$N = a'[\ln X_m/\ln X]^{1/n} \qquad (6)$$

For the monolayer thickness value employed by deBoer (*10*), $t = 3.54$ Å at $N = 1$.

The experimental information employed in this study pertains to 15 samples reported by deBoer and co-workers which encompass a large range of surface areas, average pore radii, and pore system geometry. These properties are summarized in Table 1. Experimental data from the adsorption portion of the reported isotherms were plotted according to the linearized form of Eq. (6)

$$\ln\left(\frac{t}{3.54}\right) = \left(\frac{1}{n}\right)\left[\frac{\ln X_m}{\ln X}\right] + \ln a' \qquad (7)$$

Values of apparent adsorbed layer thickness were determined from the reported BET surface area and the isotherm data, and X_m determined from a BET plot of adsorption data for $0.1 < X < 0.3$. The values of X_m were checked for consistency with the values of V_m determined.

In general, the adsorption data fit Eq. (7) quite well for low and moderate relative pressures. Deviations are noted in several cases, however, which appear to be a consequence of certain types of volume–area distributions. Positive deviations (t observed > t predicted) are observed with materials

TABLE 1
SUMMARY OF PROPERTIES OF POROUS SOLIDS

Sample[a]	S_{BET} (m^2/g)	$\bar{r} = 2V_g/S_{BET}$ (Å)	Comments on structure
A-120	609	65	Type A–Type E isotherm. Broad pore spectrum plus tubular pores with widened sections
A-450	414	99	
A-750	280	111	
MiBo-5	255	41	Type E. Tubular pores
BoW-450	92	107	Type A. Tubular pores, rectangular cross section
BoW-120	64	136	
BoG-580	66	68	Type B. Wide pores with constricted openings
BoG-750	19.1	145	
BoG-450	17.1	65	
By-250	489	20	Type B. General form of slit-shaped pores
By-270	462	21	
By-450	414	24	
By-580	245	44	
By-750	134	78	
Gibbsite-245	77	40	Slit-shaped pores

[a] Nomenclature of samples follows that of ref. *13*. Four additional samples of low surface area are reported. Their behavior is more typical of nonporous materials and they are not included here.

of moderate or large surface area and average pore size (samples A, By-580, By-750), negative deviations with materials of small average pore size or low surface area (samples BoG, By-200 to By-450). The former are normally not large, occur at $X \gtrsim 0.6$, and are attributed to the effects of a small amount of capillary condensation occurring at higher relative pressures. The latter can be significant even for $X \approx 0.3$, and indicate the existence of a number of small diameter pores which are blocked from activity, resulting in directly computed thickness values based on surface areas which are too large. For low surface area solids with small pores this effect is pronounced.

The utility of Eq. (7) in representation of adsorption data for structures of widely variant pore geometry is demonstrated in Fig. 1 for samples MiBo-5 and By-580. These two are very similar in surface area, 225 vs. 245 m^2/g, and average pore radius, 41 vs. 44 Å, but differ markedly in pore geometry, as detailed in Table 1. The plotted results for the two samples are very similar; data for the bayerite sample deviate somewhat from the linear form at higher relative pressures, but an interpretation based on information or $X < 0.5$ could make little distinction between the two.

AN EXPRESSION FOR THE ADSORBED MULTILAYER

A form of the relationship between the constants of the Halsey equation and over-

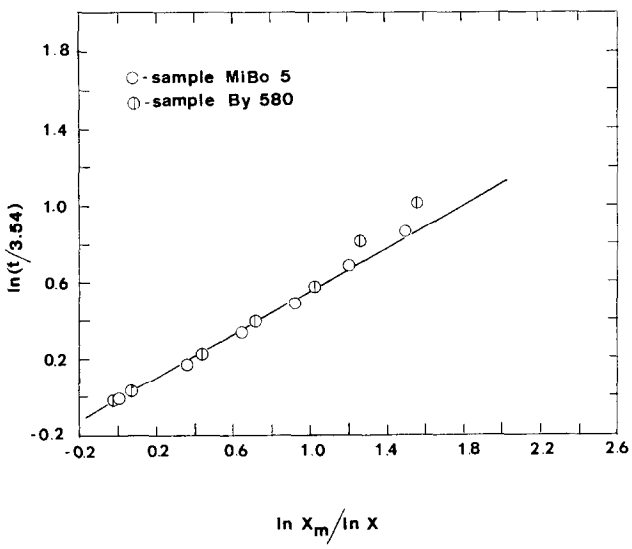

FIG. 1. Comparison of Halsey equation plot for equivalent slit and tubular pore structures.

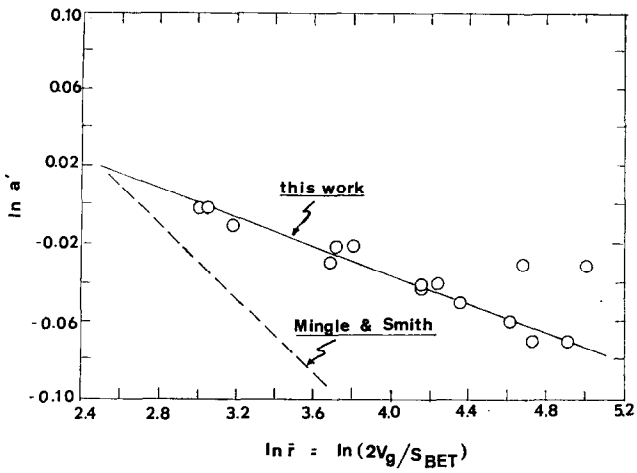

FIG. 2. Constant a' as related to average pore radius.

all properties of the solid has been suggested and discussed by Mingle and Smith (*9*). The constant, a', which represents deviation from ideal monolayer behavior, is a function of average pore radius, $\bar{r}$, suggesting that the monolayer thickness changes as the average interior surface becomes more curved. A linear variation is observed between ln a' and ln $\bar{r}$, as given in Fig. 2. The values of ln a' determined from Eq. (7) are reported in increments of 0.01 and, though some scatter results from this procedure, the results are consistent with the precision of experimental data and interpolation. The exponent, $(1/n)$, is correlated with the relative pressure at monolayer coverage, X_m, in the logarithmic plot of Fig. 3. Since X_m can be related to the value of the BET constant c, the results of Fig. 3 indicate an effect of the heat of adsorption on adsorbed layer thickness (*9*). In equation form

$$\ln a' = -(3.65 \times 10^{-2}) \ln \bar{r} + 0.11 \pm 0.01 \quad (8)$$

$$\ln (1/n) = 8.38X_m - 1.40 \pm 0.03 \quad (9)$$

The $\pm$ values are based on the maximum difference noted between experimental points and the linear representation, with the single exception of two samples of large $\bar{r}$. The form of correlation and the results obtained differ considerably from previous work, as shown in the figures.

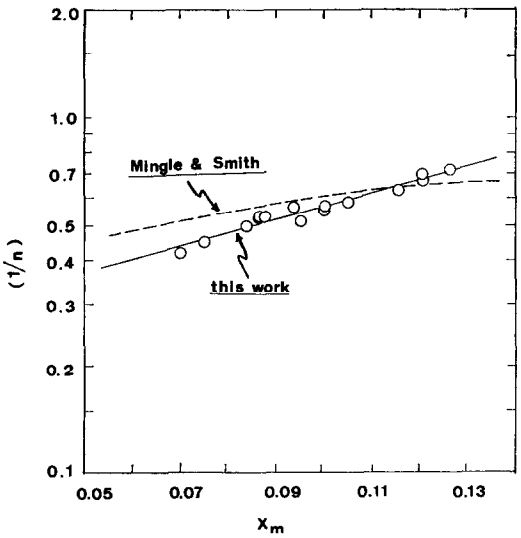

FIG. 3. Exponent of Halsey equation versus relative pressure at monolayer coverage.

CONSISTENCY OF RESULTS

It is difficult to establish suitable criteria for the evaluation of volume–area distributions, or of the procedures involved in their determination, because of the indirect means employed in measurement and computation. Comparison of surface area determined from the distribution with that obtained from BET theory is often employed, but it has been shown (*14*) that the surface area determined from volume–area distribution is a function of the geometry of the porous struc-

ture. For an assembly of constricted, tubular (ink bottle) pores, $S_{des} > S_{BET}$, while $S_{ads} = S_{BET}$; for a regular and open structure such as an assembly of slit-shaped pores, $S_{des} = S_{BET}$ and $S_{ads} < S_{BET}$. Surface areas determined from the pore-size distribution are almost always those based on desorption data; if these two types of pore geometry are visualized as representative of two extremes of behavior, then surface areas from the distribution cannot be smaller than S_{BET}, but they may be larger.

The consistency of the proposed correlation is illustrated below with two examples which yield, with other methods, $S_{des} < S_{BET}$. This violation of the surface area restriction often seems to be associated with porous structures in which (a) the average pore radius is small (<50 Å) and (b) the relative pressure corresponding to monolayer coverage is low (<0.10). In Fig. 4 is given a comparison of multilayer thickness estimated by four methods for a silica gel sample studied by Dollimore and Heal (*3*). S_{des} computed with Eq. (3) was 570 m²/g, S_{des} with the Shull correlation 710 m²/g, and

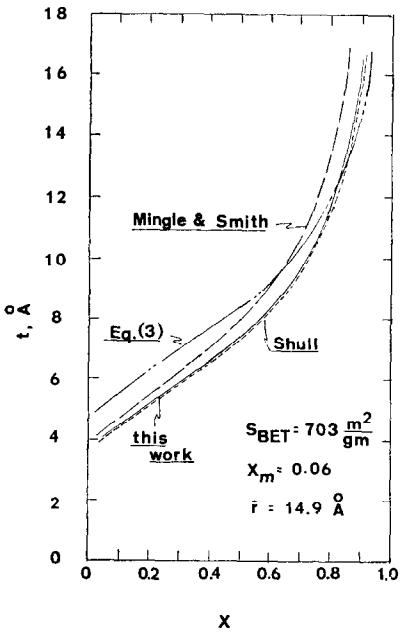

FIG. 4. Comparison of adsorbed layer thickness predictions for silica gel sample of Dollimore and Heal (*3*).

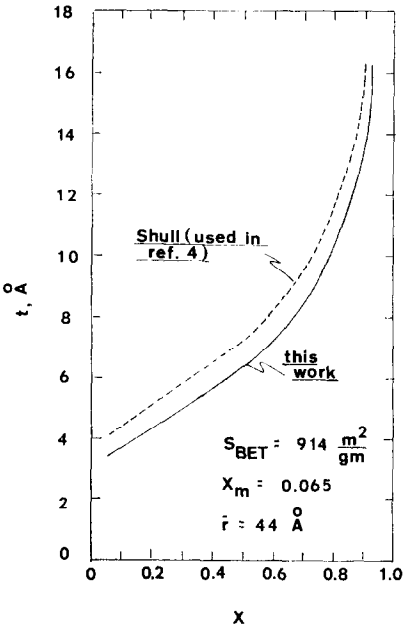

FIG. 5. Comparison of adsorbed layer thickness predictions for aerogel sample of Anderson (4).

S_{BET} 705 m²/g. S_{des} using the Mingle and Smith correlation was not computed rigorously for this case, but was estimated to be about 620 m²/g. The Shull correlation is the only one of these which does not result in violation of $S_{des} \geq S_{BET}$; the predictions of the present work fall within about 1% of the Shull values, thus surface area results with this correlation are in good agreement with S_{BET}.

Figure 4 also illustrates the proportionality between differences in thickness correlations and differences in surface areas computed from them. For example, in the test sample most of the surface area is contained in capillaries of radius below 35 Å, or $X < 0.6$; the Shull correlation is some 20% lower than that of Eq. (3) in this region, whereas the computed areas also differ by 20%. This proportionality appears applicable so long as comparison is made between correlations of similar shape in the range of X corresponding to the majority of internal area, and allows convenient comparison of surface area results for the different methods.

A second comparison is given in Fig. 5 for an aerogel sample reported by Anderson (*4*).

The value of S_{des} reported (employing the Shull values) was 820 m²/g, about 10% smaller than S_{BET} of 914 m²/g. The estimation of this work is similar in shape over the entire range of relative pressure and falls about 15% below the Shull values, giving an estimated S_{des} of 940 m²/g.

Adsorbed Layer Effects on the Adsorption–Desorption Isotherm

The shape of adsorption–desorption isotherms may be affected by the adsorbed multilayer, particularly at low relative pressures. This is a consequence of both the magnitude and rate of change of thickness, which varies widely for differing structures. From Eq. (6)

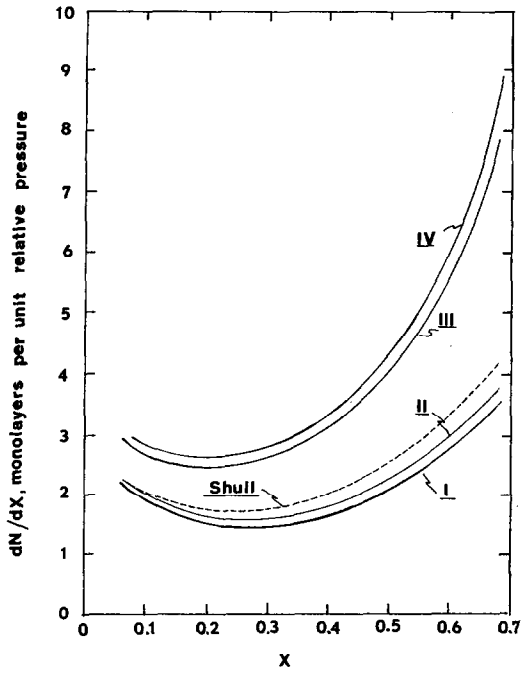

Fig. 6. Rate of change of adsorbed layer thickness with relative pressure: I, low $(1/n)$, low a'; II, low $(1/n)$, high a'; III, high $(1/n)$, high a'; IV, high $(1/n)$, low a'; Ranges: $0.43 \leq (1/n) \leq 0.70$; $0.932 \leq a' \leq 1.00$.

$$\frac{dN}{dK} = -\frac{a'}{nX(\ln X_m)}\left[\frac{\ln X_m}{\ln X}\right]^{1/n+1} \quad (10)$$

These rates are compared with those predicted from the Shull correlation in Fig. 6 for a range of values of a' and $(1/n)$. Case III represents a type of structure particularly susceptible to such effects; these structures typically contain an important fraction of their volume and area in small pores which may be rendered inactive for adsorption through blocking by the adsorbed multilayer. This behavior is observed for several of the samples of Table 1 and has been referred to previously in terms of an apparent negative deviation from the prediction of Eq. (7).

Acknowledgment

This research was supported by the National Science Foundation and the Petroleum Research Fund, administered by the American Chemical Society.

References

1. Barrett, E. P., Joyner, L. G., and Halenda, P. P., *J. Am. Chem. Soc.* **73**, 373 (1951).
2. Innes, W. B., *Anal. Chem.* **29**, 1069 (1957).
3. Dollimore, D., and Heal, G. R., *J. Appl. Chem.* **14**, 109 (1964).
4. Anderson, R. B., *J. Catalysis* **3**, 50 (1964).
5. Irving, J. P., and Butt, J. B., *J. Appl. Chem.* **15**, 139 (1965).
6. Shull, C. G., *J. Am. Chem. Soc.* **70**, 1405 (1948).
7. Pierce, C., *J. Phys. Chem.* **57**, 64, 149 (1953).
8. Cranston, R. W., and Inkley, F. A., *Advan. Catalysis* **9**, 143 (1957).
9. Mingle, J. O., and Smith, J. M., *Chem. Eng. Sci.* **16**, 31 (1960).
10. Lippens, B. C., Linsen, B. G., and deBoer, J. H., *J. Catalysis* **3**, 32 (1964).
11. Halsey, G., *J. Chem. Phys.* **16**, 931 (1948).
12. deBoer, J. H., and Lippens, B. C., *J. Catalysis* **3**, 38 (1964).
13. Lippens, B. C., and deBoer, J. H., *J. Catalysis* **3**, 44 (1964).
14. deBoer, J. H., Van den Heuvel, A., and Linsen, B. G., *J. Catalysis* **3**, 268 (1964).